Electronic Supplementary Material (ESI) for Journal of Materials Chemistry A.

Supplemental Materials

Defect Accumulation in Swift Heavy Ion-Irradiated CeO_2 and ThO_2

Raul I. Palomares[1], Jacob Shamblin[1,2], Cameron L. Tracy[3], Joerg Neuefeind[4], Rodney C. Ewing[3], Christina Trautmann[5,6], Maik Lang[1]

1. Department of Nuclear Engineering, University of Tennessee, Knoxville, Tennessee 37996, USA

2. Department of Physics and Astronomy, University of Tennessee, Knoxville, Tennessee 37996, USA

3. Department of Geological Sciences, Stanford University, Stanford, California 94305, USA

4. Chemical and Engineering Materials Division, Spallation Neutron Source, Oak Ridge National Laboratory, Oak Ridge, Tennessee 37831, USA

5. GSI Helmholtzzentrum für Schwerionenforschung, 64291 Darmstadt, Germany

6. Technische Universität Darmstadt, 64287 Darmstadt, Germany

Corresponding Author: mlang2@utk.edu

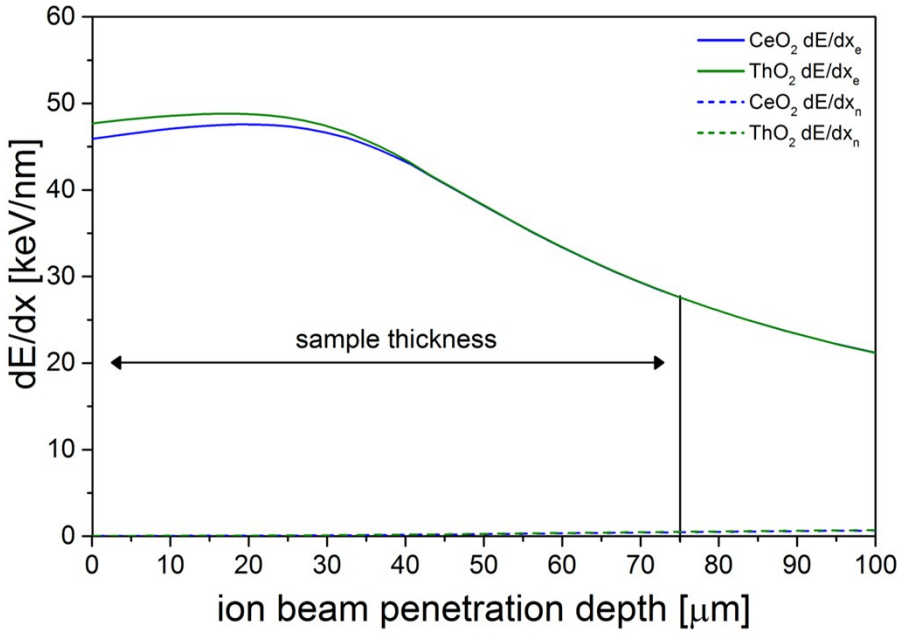

Supplemental Figure 1: Linear energy loss as a function of ion penetration depth in CeO_2 and ThO_2 calculated by SRIM-2010 [1]. The average electronic energy loss (*solid lines*) across the sample thickness (~75 μm) is 41 keV/nm and 42 keV/nm for CeO_2 and ThO_2, respectively. The corresponding nuclear energy loss (*dashed lines*) is negligible.

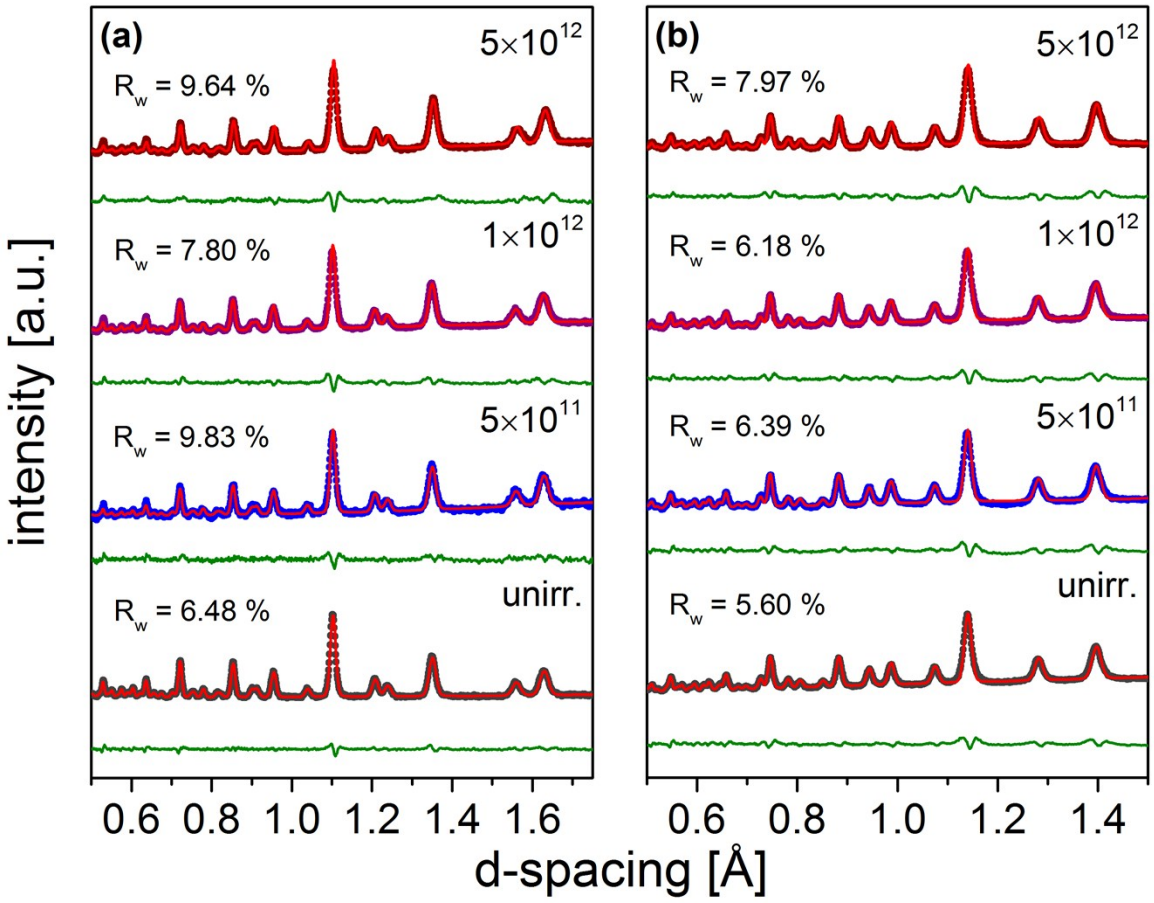

Supplemental Figure 2: Refined neutron diffraction patterns for all (a) CeO_2 (b) ThO_2 samples. The measured data, fitted profiles, and difference curves are represented by the colored circles, solid red lines, and solid green lines, respectively. Only the diffraction patterns from the $\theta = 66°$ detector are shown for brevity. The fluence values are provided above each diffraction pattern.

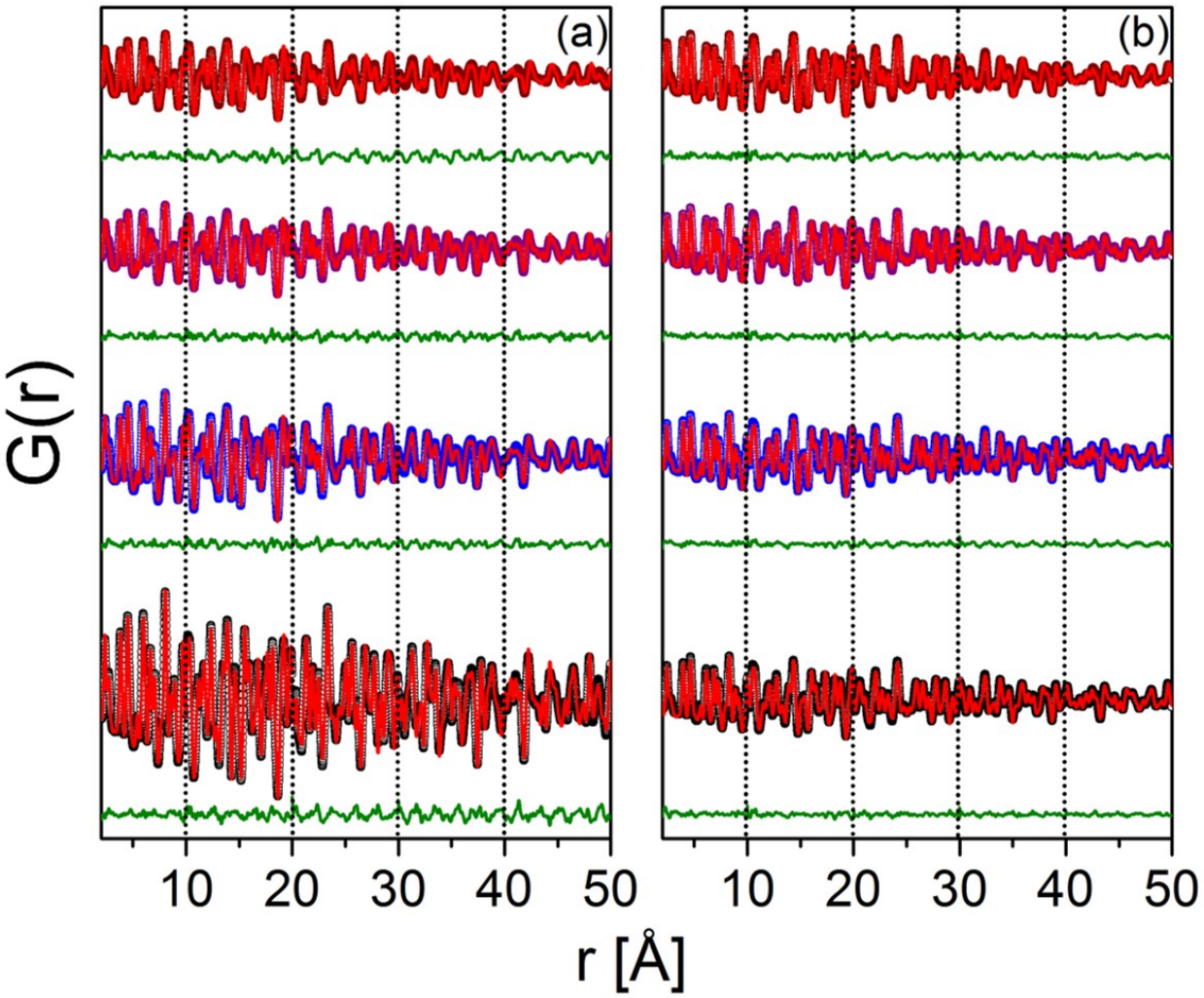

Supplemental Figure 3: Refined pair distribution functions (PDFs) for all (a) CeO_2 and (b) ThO_2 samples. The measured PDFs, fitted fluorite structure models, and difference curves are represented by the colored circles, solid red lines, and solid green lines, respectively. The boundaries for the boxcar fits are denoted by the vertical, dotted black lines. The fits are representative of the ~10 Å-wide boxcar fits. Note: the four PDFs for a given material are not normalized to the same intensity; therefore, larger difference curves in this figure do not necessarily imply a larger R_w value. For a comparison of R_w values, refer to Figure 4 in the text.

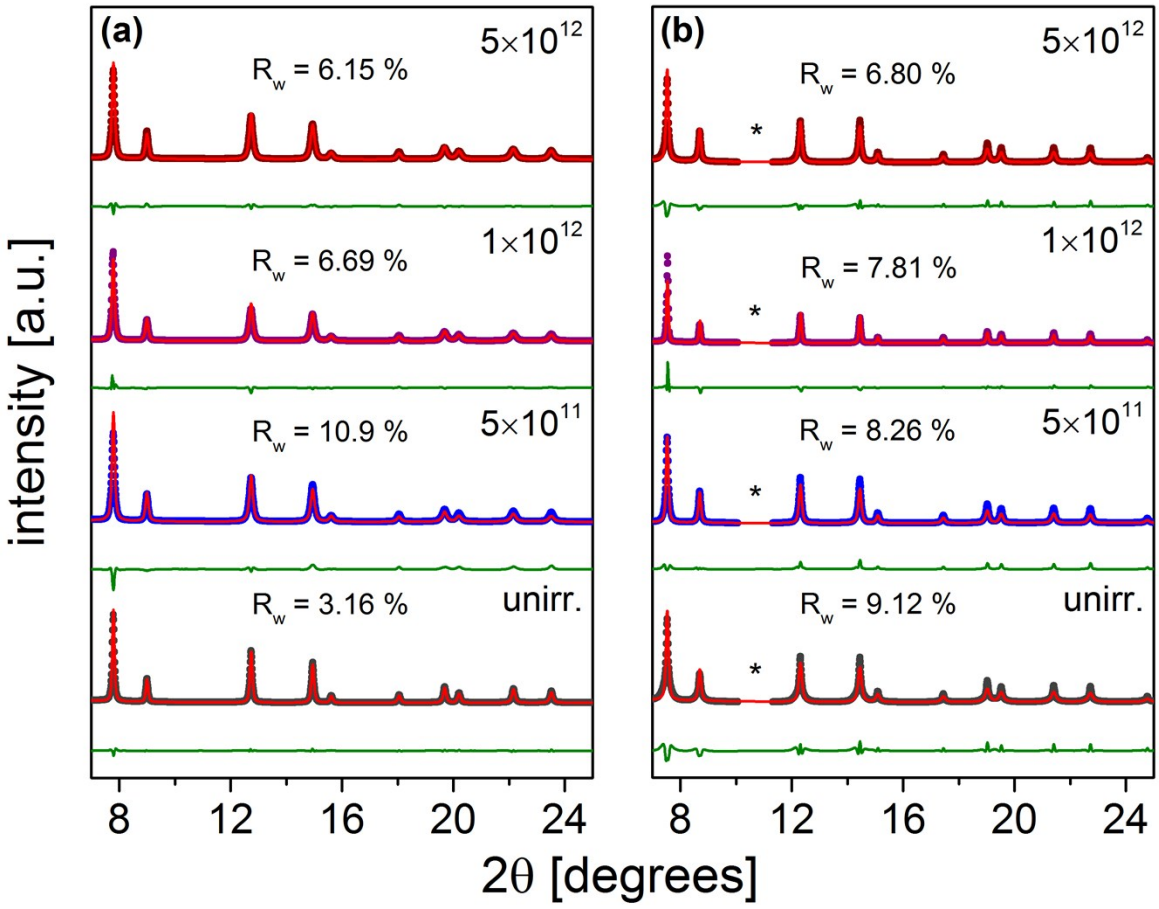

Supplemental Figure 4: Refined synchrotron X-ray diffraction (XRD) patterns for all samples. The measured data, fitted profiles, and difference curves are represented by the colored circles, solid red lines, and solid green lines, respectively. The XRD peaks are much sharper compared to the Bragg peaks in the neutron diffraction patterns. This enabled the determination of more accurate unit cell parameters.

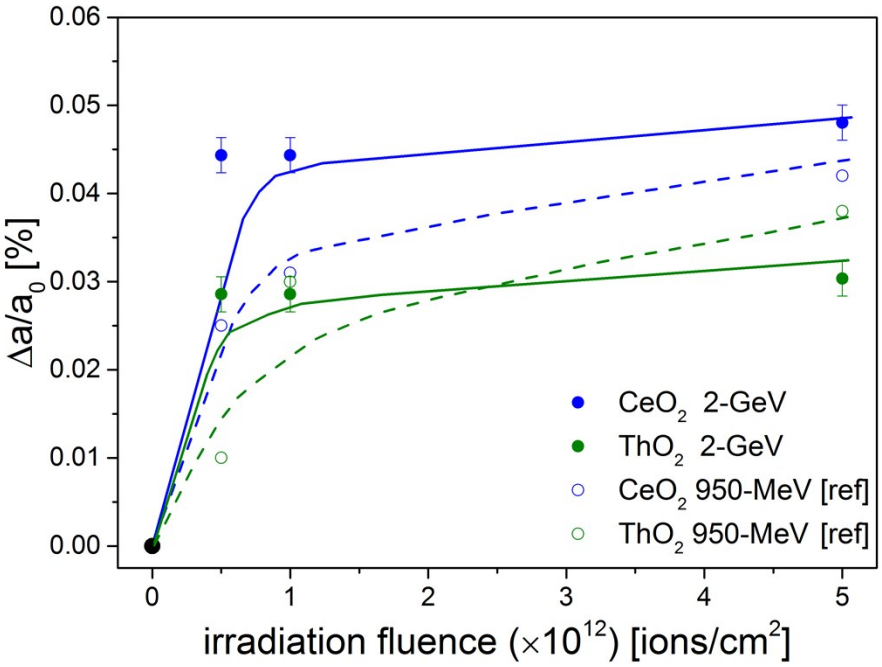

Supplemental Figure 5: Relative change in unit cell parameter, $\Delta a/a_0$, as a function of irradiation fluence as determined by Rietveld refinement of the X-ray diffraction patterns. The unit cell parameters obtained from X-ray and neutron diffraction are in agreement within experimental uncertainty. The lines are guides to the eye. The data are compared to data published for CeO_2 and ThO_2 samples irradiated with 950 MeV Au ions [2]. Both data sets illustrate similar irradiation behavior, albeit with different damage accumulation rates.

Supplemental Table 1: Interatomic distances derived from the pair distribution functions. The values represent the mean first nearest-neighbor cation-oxygen (<C-O>), oxygen-oxygen (<O-O>), and cation-cation (<C-C>) distances.

sample	<C-O>	<O-O>	<C-C>
CeO_2 unirradiated	2.344(1) Å	2.711(1) Å	3.831(1) Å
CeO_2 5×10^{11}	2.332(1) Å	2.694(2) Å	3.829(1) Å
CeO_2 1×10^{12}	2.293(10) Å	2.716(5) Å	3.837(1) Å
CeO_2 5×10^{12}	2.349(2) Å	2.717(2) Å	3.837(1) Å
ThO_2 unirradiated	2.419(1) Å	2.822(1) Å	3.960(1) Å
ThO_2 5×10^{11}	2.423(1) Å	2.784(1) Å	3.960(1) Å
ThO_2 1×10^{12}	2.421(1) Å	2.810(1) Å	3.961(1) Å
ThO_2 5×10^{12}	2.425(1) Å	2.784(1) Å	3.960(1) Å

References

1. J. F. Ziegler, M. D. Ziegler and J. P. Biersack, *Nuclear Instruments & Methods in Physics Research Section B-Beam Interactions with Materials and Atoms*, 2010, **268**, 1818-1823.
2. C. L. Tracy, M. Lang, J. M. Pray, F. Zhang, D. Popov, C. Park, C. Trautmann, M. Bender, D. Severin, V. A. Skuratov and R. C. Ewing, *Nat Commun*, 2015, **6**, 6133.